Journal of the European Ceramic Society 20 (2000) 489–495

A preliminary study of stress-assisted fluid penetration in ceramic bricks

S.I. Marras [a], I.A. Ihtiaris [a], N.K. Hatzitrifon [b], K. Sikalidis [c], E.C. Aifantis [a,d,*]

[a] *Laboratory of Mechanics and Materials, Polytechnic School, Aristotle University of Thessaloniki, 54006 Thessaloniki, Greece*
[b] *4th Superintendance for Modern Monuments /The Hellenic Ministry of Culture, 17, Herodotou Str. 54634 Thessaloniki, Greece*
[c] *Department of Chemical Engineering, Aristotle University of Thessaloniki, 54006 Thessaloniki, Greece*
[d] *Center of Mechanics of Materials and Instabilities, Michigan Technological University, Houghton, MI 49931, USA*

Received 18 January 1999; received in revised form 8 June 1999; accepted 3 July 1999

Abstract

Solid bricks manufactured using clays from Thessaloniki area have been analysed by X-ray powder diffraction and their mineralogical composition showed the presence of chlorite, muscovite, quartz, and albite. The compressive strength values of dried and wetted bricks were determined and a decrease of about 25% was observed for water saturated bricks. Using mechanical extensiometers, stress strain diagrams and Poisson ratios were measured. In order to model the liquid diffusion through the brick and the chemomechanical damage due to the coupled action of liquid presence and applied loads, the front of a penetrating solute has been mathematically expressed by using Aifantis'stress-assisted diffusion theory. Pre-loaded bending specimens were sprayed with a liquid. After a certain time the specimens were loaded until fracture. Different phenomenological constants of the stress-assisted diffusion theory have been assumed for the compression and tension regime and a satisfactory agreement between theoretical predictions and experimental data has been obtained.

Keywords: Bricks; Strength; Water penetration; X-ray methods

Zusammenfassung

Vollziegel, produziert aus Lehm von der Gegend um Thessaloniki, wurden durch die Diffraction von X-Wellen an Steinmehl analysiert. Ihre mineralogische Zusammetsetzung zeigte die Presenz von Chlorid Muscovit, Quarz und Albit. Die Druckfestigkeit von trockenen und nassen Ziegeln wurde ermittelt, wobei die mit Wasser gesaettigten Ziegel einen ungefaer 25% niedrigeren Wert als die trockenen zeigten. Mit mechanischen Dehnungsmessern wurden die Spannungs- Dehnungsdiagramme gefertigt und die Poisson'she Zahl ermittelt. Die Diffusion der Fluessigkeit durch einen Ziegelstein, sowie der durch die gleichzeitige Anwesenheit von Fluessigkeit und Belastung chemo-mechanische Zerfall, sollte modeliert werden. So wurden die Theorie von Aifantis ueber die spannungsunterstuetzte Diffusion angewandt, um die Front der penetrierenden Substanz mathematisch auszudruecken. Vorbelastete Proben wurden mit einer Fluessigkeit bespritzt und nach gewisser Zit bis zum Bruch belastet. Fuer die Zug- und Druckzone wurden verschiedene phenomenologische Konstanten nach der spannungsunterstuetzten Diffusionstheotie ermitteit wobei eine zufriedenstellende Uebereistimmung zwischen theoretischer Analyse und experimentellen Ergebnissen erreicht wurde.

1. Introduction

Environmental agents penetrating solid components under load, reduce the material strength. In particular, this was studied empirically for bricks[1–3] and also for other building materials.[4,5] For the interpretation of such chemomechanical phenomena a stress-assisted diffusion theory has been developed by Aifantis.[6–9] According to this theory the concentration distribution of a solute may eventually be expressed as a function of the hydrostatic stress induced by the external load. This expression also involves two material constants α and β which depend on the diffusivity and the chemo-stress effect.

For the determination of these two constants studies have been made for different materials. For example, Unger et al.[10] determined α in various materials underlying tension and correlated it with the flow stress which, in

* Corresponding author. Tel.: +30-031-995-921; fax: +30-031-995-921.

0955-2219/00/$ - see front matter
PII: S0955-2219(99)00186-7

turn, is strongly dependent on the microstructure. Papadopoulos[11] also presented an overview for the values of both constants for several materials in tension, in relation to the problem of environmental fracture.

In this work, the mineralogical composition and the mechanical properties of the bricks used were determined including stress-strain diagram, modulus of elasticity, Poisson ratio, wet and dry compressive strength. Next, the front of a diffusive solute was determined experimentally and modelled mathematically. The characteristic values α and β of Aifantis' stress-assisted diffusion theory were experimentally estimated. The results indicate that these constants have different values in the compressive and tensile area of the brick. This issue will be addressed separately in a future publication.

2. Materials and methods

The solid bricks samples used were prepared by powder pressing. The powder was prepared through dry processing and mixing of two clays. The clays were dried, and lump breaking, with mixing-milling and sieving followed. The mixture of the powder was humidified and formed by pressing in the shape of bricks. The mineralogical composition of the mixture was carried out by X-ray powder diffraction (XDR) using a Philips Model PW 1830 diffractometer. The shaped bricks were subjected to thermal treatment. The firing was performed to a peak temperature of 1080°C in a tunnel kiln following a common firing procedure for these products.

For the study of the effect of moisture content on the compressive strength (according to A.S.T.M. C 67-92a), every brick was cut into three part-specimens (A,B,C) by diamond slow cutting and their dimensions were measured. Then the specimens were dried at 115°C for 24 h. One of the three specimens (A) was submerged in clean water for about 24h and boiled for 5 hours. The water saturated specimens were wiped off and weighted within 5 min after its removal from the bath. In this way the water absorption was obtained. The compressive strength of the specimens was determined by using a Mohr & Federhaff, Model 5359 test machine.

For the experimental determination of Poisson's ratio and Young's modulus of the bricks, the test specimens were subjected to five successive loading steps, measuring the corresponding strain along the direction of the applied load and the transverse strain, by using mechanical extensiometer with an accuracy of 1 μm.

Finally, the stress-assisted diffusion process of a fluid agent was studied experimentally. For this purpose the following experiment as steps were followed:

- The specimen was subjected to a three-point bending configuration with a concentrated force, equal to the 3/4 of its expected value for fracture, as shown in Fig. 1. In order to avoid failure at an accidental point or at the fastens, the specimen was pre-cracked in the tensile area ($x = 1/2$) so that the maximum stresses would develop in the loaded axis. The sprayed surface x-z (Fig. 1) in which bending, tensile and compressive, stresses are developed, was placed horizontally; so the spraying liquid was not able to migrate from the compressive to the tensile area.
- While under pressure, the specimen's surface was sprayed by a red colored penetrating substance (Helling by Lux Nr 201), uniformly.
- The loading was kept for a certain time (5 min), so that the penetration of the substance through the brick's pores can take place. Then the load was increased until fracture in two pieces took place.
- The fracture surface of the specimen was sprayed by a white spray (Helling Net-L-Chek D70), in order for the red coloured substance to emerge from the pores of the specimen. In this way the white penetrating liquid became pink and the area that absorbed the penetrating liquid, was exposed.

3. Results and discussion

The mineralogical analysis showed the presence of chlorite, muscovite, albite and quartz as dominant minerals. This is the typical mineral composition of solid bricks manufactured in Thessaloniki area.

The results of the water absorption values in the eight specimens (A) and the relevant values of the compressive strength in the eight wetted specimens (A) and the sixteen dry ones (B, C) are given in Tables 1 and 2.

According to these results every saturated specimen has lower strength than the two dry specimens of the same brick.

Fig. 2 shows the relation between compressive strength and water absorption.

The results of the measurements pertaining to the determination of Poisson's ratio and Young's modulus, are shown in Tables 3 and 4. (The specimens were loaded in the z axis).

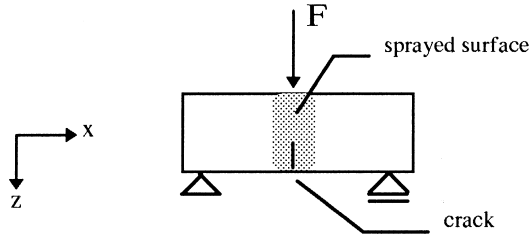

Fig. 1. The three-point bending configuration. The x-z plane is horizontal, i.e. parallel to the ground.

Table 1
Water absorbtion and compressive strength of bricks No 1,2,3,4

Specimen	1A	1B	1C	2A	2B	2C	3A	3B	3C	4A	4B	4C
Water absorption %	7.68			8.11			8			8.8		
Compressive strength (N/mm^2)	21.3	26.8	29.84	19.5	26.9	25.9	20.1	28.86	30.64	16.7	26.4	23.84
% Variation[a]	−24.7			−26.1			−32.4			−33.6		

[a] % Variation of the compressive strength of the water saturated specimen A, from the average of the compressive strength of the two dried specimens, B and C.

Table 2
Water absorption and compressive strngth of bricks No 5,6,7,8

Specimen	1A	1B	1C	2A	2B	2C	3A	3B	3C	4A	4B	4C
Water absorption %	6.8			8.5			7.02			7.5		
Compressive strength (N/mm^2)	28.45	31.4	34.3	17.2	22.6	24.5	25.3	30.4	31.4	22.1	27.5	28.3
% Variation[a]	−13.4			−27			−18			−20.8		

[a] % Variation of the compressive strength of the water saturated specimen A, from the average of the compressive strength of the two dried specimens, B and C.

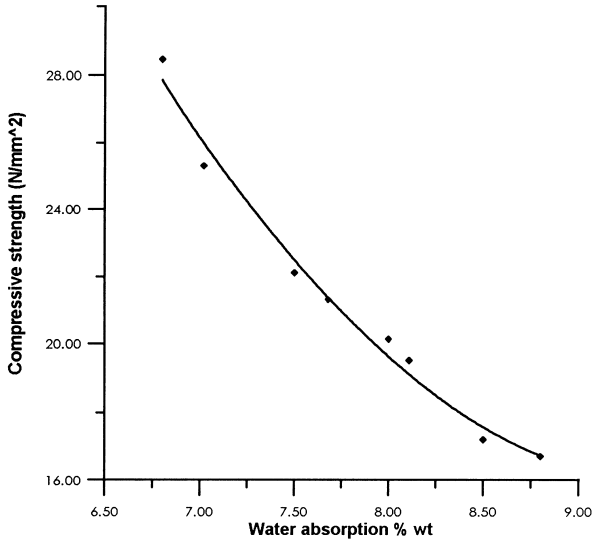

Fig. 2. Relationship between compressive strength and water absorption.

Using pairs of stress and corresponding strain values, the following stress–strain diagram was obtained (Fig. 3).

From the slope of the above diagram, in the linear elasticity regime the value of Young's modulus of E≈16055 N/mm^2 is obtained. From the values of the lateral strains ε_y and ε_z, the value of the corresponding Poisson's ratio ($\nu = -\varepsilon_y/\varepsilon_z$) is determined as $\nu = 0.21$.

Next, we turn to the fluid infiltration properties of the bricks. Fig. 4 is a photograph resulted from the experimental measurements after fracture took place. It shows the fracture surface (y–z plane, x = L/2) of the brick where the penetration depth of the diffusive liquid can be observed (marked by the arrows).

Table 3
Measurements of the specimen 1: [Dimensions (cm)/(x,y,z) = (3, 10.85, 11.1)]

Stress (N/mm^2)	0	2	4	6	8	10
$\varepsilon_y(\times 10^{-4})$	0	0.24	0.49	0.73	1.44	2.7
$\varepsilon_z(\times 10^{-4})$	0	1.2	2.3	3.48	6	9
ν	–	0.20	0.217	0.21	0.24	0.3

Table 4
Measurements of the specimen 2: [Dimensions (cm)/(x,y,z) = (3, 10.7,11.1)]

Stress (N/mm^2)	0	2	4	6	8	10
$\varepsilon_y(\times 10^{-4})$	0	0.276	0.59	0.92	1.82	3.616
$\varepsilon_z(\times 10^{-4})$	0	1.38	2.74	4.2	7.01	11.3
ν	–	0.20	0.215	0.22	0.26	0.32

Within a simple strength of materials approach, the distribution of the normal stresses in the beam can approximately be estimated as shown in Fig. 5. (A more accurate determination would involve a numerical factor determined by the geometric characteristics of the beam and the notch. However this correction is not essential for the semi-quantitative results to be presented below).

The following strength of materials estimates for the beam stresses hold:

$$\sigma_y \approx \sigma_z \approx= 0, \sigma_x = \frac{M_y}{I_y} z = \frac{3FL}{bh^3} z \quad (1)$$

where M_y is the bending moment, I_y is the moment of inertia, F is the applied load and L, b, h are the length, the width, and the height of the beam ($-h/2 \leqslant z \leqslant h/2$).

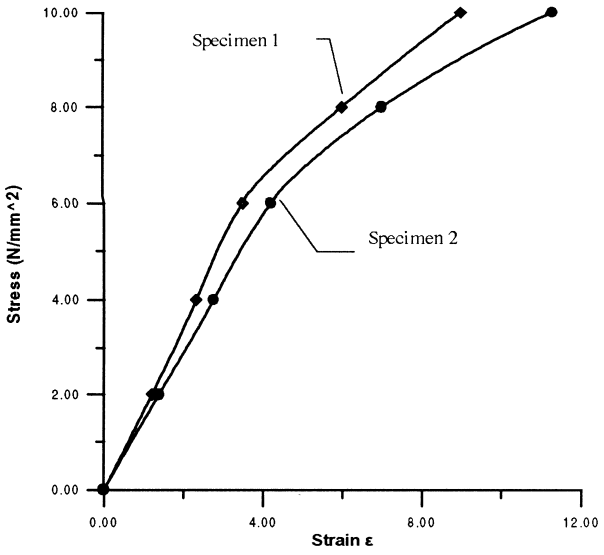

Fig. 3. Stress–strain diagram of the specimen 1 and 2 (bricks).

In Fig. 6 the diffusion front of the fluid on the y–z plane, as determined from the photograph of Fig. 4, is shown. Dots denote the experimental recordings which in the present case are twenty in number ($K = 20$). Mathematically, the front can be described by a fitted curve utilising a number of the curve's points ($K > R$). With an iteration method based on the least square technique, i.e. Levenberg-Marguart algorithm, the value of the unknowns can be calculated. The simplest way of representing this front is by a straight line. The corresponding equation is $y = 0.19 + 0.03z$, and the error is $s = 0.008$. Two different straight lines, one for the tensile and one the compression regime give the equations $y = 0.23 + 0.05z$ and $y = 0.21 + 0.022z$, respectively, with an error $s = 0.001$.

In order to model the process of fluid penetration, the Aifantis' stress-assisted diffusion theory is used. The derivation of this theory[6–9] rests upon the balance of mass and momentum and related constitutive assumptions. The governing equation read:

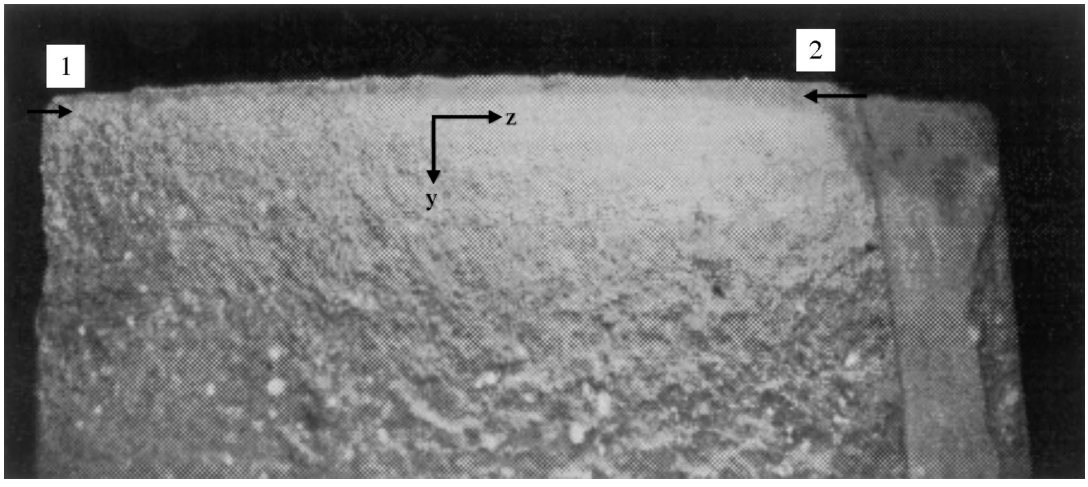

Fig. 4. Fractured surface (y–z, x = L/2) of a brick under the influence of stress assisted diffusion 5 min after exposure to the fluid. (1): point of maximum compression in x-direction (and minimum liquid absorption); (2): point of maximum tension in x-direction (and maximum liquid absorption).

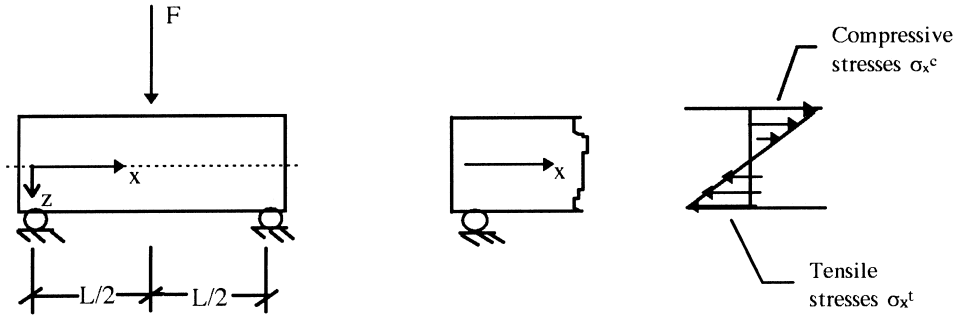

Fig. 5. Distribution of normal stresses in bending.

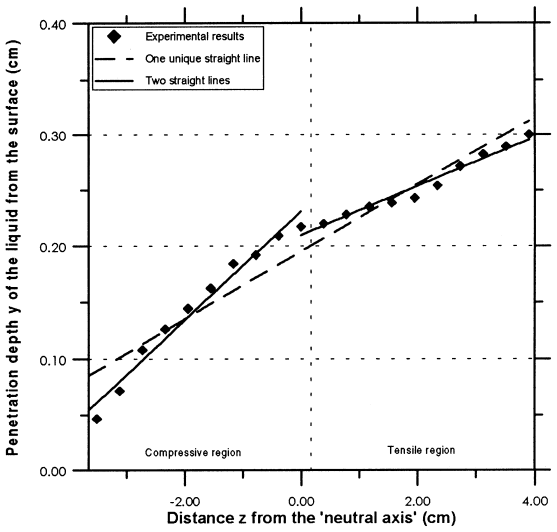

Fig. 6. The experimental data of the penetrating front in the y-z plane five minutes after exposure to the fluid. The front is represented by a single straight line or by two straight lines.

$$\rho_t + \mathrm{div} j = 0 \tag{2}$$

$$j = -(D + N\sigma)\mathrm{grad}\rho + M\rho\mathrm{grad}\sigma \tag{3}$$

$$\mathrm{div} S = 0 \tag{4}$$

where ρ is the concentration of the diffusive species, the subscript t denotes differentiation with respect to time, j is the mass flux of the diffusive substance; D, M, N, are phenomenological constants with their physical meaning discussed in[6,10], S is the stress tensor of the solid, and σ is the hydrostatic stress. When Eq. (3) is substituted into Eq. (2) the following stress-assisted diffusion equation is obtained

$$\rho_t = (D + N\sigma)\nabla^2\rho - (M - N)\mathrm{grad}\sigma.\mathrm{grad}\rho \tag{5}$$

where $\nabla^2\sigma = 0$ in an uncoupled theory where the mechanical equations of equilibrium [Eq. (4)] can be solved independently together with the equations of elasticity and compatibility of the solid matrix to determine $\boldsymbol{S}$. This equation generalises Cottrell's stress-assisted diffusion theory in replacing the constant diffusivity D by an effective one $D^{\mathrm{eff}} = D + N\sigma$ dependent linearly on the hydrostatic stress. For $j = 0$, the corresponding equilibrium solution reads

$$\rho = \rho_o(1 + \beta\sigma)^{\alpha} \tag{6}$$

where $\alpha = M/N$, $\beta = N/D$ and ρ_o is a reference concentration. Values of α and β have been provided in[10,11] only for material regions under tension.

Since the process of liquid penetration cannot obviously be modelled by a time-independent process, one would need to solve the transient form of Eq. (5) under the condition of constant stress gradient which is the case for the present bending configuration. Such solutions do exist (see Wilson and Aifantis[8]) but they are not convenient to implement in the present problem. Since only semi-quantitative results are desired we will follow a simpler approach by neglecting the effect of the stress gradient of Eq. (5) and consider the transient process by retaining the stress-dependent effective diffusivity term. Thus, we have

$$\rho_t = \rho D^{\mathrm{eff}}\nabla^2\rho \tag{7}$$

or, in one dimension

$$\rho_t = D^{\mathrm{eff}}\nabla^2_{yy}\rho \tag{8}$$

The solution of this differential equation for finite source (thin film) boundary condition is

$$\rho(y, t) = \frac{\rho^o}{\sqrt{4D_{\mathrm{eff}}t}}\exp\left[-\frac{y^2}{4D_{\mathrm{eff}}t}\right] \tag{9}$$

where ρ_o is the source strength (initial amount of mass at the origin).

From these equations it follows that the characteristic diffusion depth is given by the expression

$$y = 2\sqrt{D_{\mathrm{eff}}t} \tag{10}$$

or

$$y = 2\sqrt{(D + N\sigma)t} \tag{11}$$

which can be used for estimating the front of the penetrating fluid.

Thus, by using Eq. (1), Eq. (11) reads

$$y = 2\sqrt{\left(D + N\frac{3FL}{bh^3}z\right)t} \tag{12}$$

For $t = 5$ min and the given values of F, L, b, h (2.3 N/mm^2, 20.3 cm, 6.6 cm, 7.8 cm) we can fit the experimental points depicted in Fig. 6 by Eq. (12). Instead of the straight lines shown in Fig. 6, the two curves shown in Fig. 7 are obtained. The values of the constants D and N associated with this fitting are given below.

- In the compressive region: $D_c = 3.91 \times 10^{-5}$ cm^2/sec
  and
  $N_c = 2.56 \times 10^{-6}$ cm^4/(N sec)
  $\beta_c = \dfrac{N_c}{D_c} = 6.53$ mm^2/N

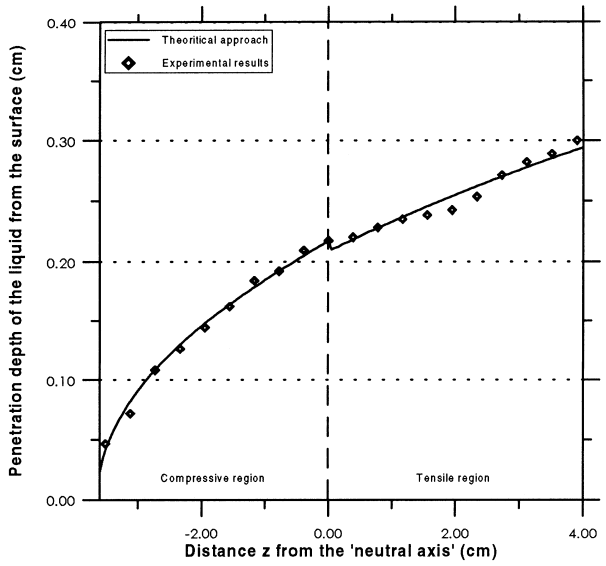

Fig. 7. Description of the front using Eq. (12) separately for the tension and the compression regimes.

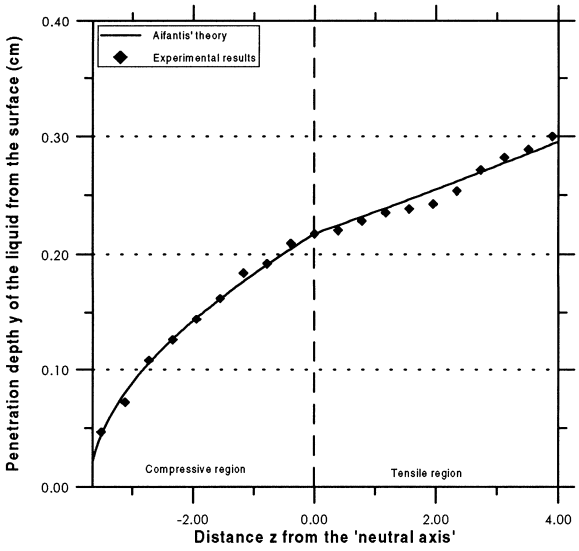

Fig. 8. Description of the front using Eq. (13) for the tension and the compression area.

• In the tensile region: $D_t = 3.61 \times 10^{-5}$ cm^2/sec and $N_t = 2.04 \times 10^{-6}$ cm^4/(N sec) $\beta_t = \dfrac{N_t}{D_t} = 5.65$ mm^2/N

The error is $s = 7.4 \times 10^{-4}$.

This method does not provide a value for the constant α entering into the equilibrium solution given by Eq. (6). To utilise this solution we make the additional hypothesis that the concentration ρ is related linearly with the diffusion depth. The validity of this ad hoc assumption can only judged by the conclusions to which leads as will be seen below. The concentration of the fluid due to the brick absorption on the neutral axis of the beam (where the normal stress σ_x is zero) is ρ_o. Moreover, it is assumed that only after a material point has reached the final equilibrium concentration $\rho_z = \rho$, a point next to can accumulate fluid and, thus, the diffusion front propagates step by step.

Thus, by substituting Eq. (1) into Eq. (6), we obtain:

$$\rho = \rho_o \left[1 + \beta \frac{3FL}{bh^3} z \right]^{\alpha} \tag{13}$$

With the aforementioned assumptions Eq. (13) can be used to model the fluid front. Since all quantities, but the parameters α and β, entering Eq. (13) are known (i.e. the values of $F = 2.3N$/mm^2, $L = 20.3$ cm, $b = 6.6$ cm, $h = 7.8$ cm) the experimental points of the front given in Fig. 6 are fitted by the graph shown in Fig. 8 with the following values for α and β.

• in the compressive region (tr$\sigma < 0$): $\beta_c = 6.42$ mm^2/N, $\alpha_c = 0.53$

• in the tensile region (tr$\sigma > 0$): $\beta_t = 5.2$ mm^2/N, $\alpha_t = 0.45$

The error is $s = 8.2 \times 10^{-4}$. It follows that the value of the constant β obtained by the two methods are comparable.

4. Conclusions

Mechanical and fluid penetration properties of a building brick material consisted of muscovite, chlorite, quartz, albite was considered. The compressive strength was experimentally estimated as $\sigma = 29$ kN/mm^2, the Young's modulus $E = 16055$ N/mm^2 and the Poisson's ratio $\nu = 0.21$. Diffusion properties of a penetrating liquid and the corresponding front in a brick subjected to bending stresses was also considered and interpreted by using a simplified version of a stress assisted diffusion theory and simplified strength of materials approximations. In future work, the introduced simplifying assumption of the stress-assisted diffusion theory will be relaxed and additional experimental measurement will be performed. Different sizes of brick specimens will be used, optical microscopes observation will be performed, a radioactive substance will be employed for more accurate estimates of the penetration front and a theoretical model for the strength dependence the water absorption will be developed.

Acknowledgements

Financial support under the Ministry of Culture of Greece grant No 8515, PENED99 grant No 99-ED546

is acknowledged. Discussion with D.A. Konstantinidis on the stress-assisted diffusion analysis and the help of D. Tripopoulos with the mechanical tests are also gratefully acknowledged. Part of these results were obtained by the first two authors in the course of completing their diploma thesis.

References

1. Egermann, R., Structural Conservation of Stone Masonry. *Proceedings of the Int. Techn. Conf.* in Athens, ICCROM, Rome, 1990.
2. Papayanni, I., A holistic way of studying mortars and bricks of ancient masonries for manufacturing compatible repair materials. *Proc. 4th International Symposium on the Conservation of Monuments in the Mediterranean*, Ed. Technical Chamber of Greece, Scient. Editors: A. Moropoulou, F. Zezza, E. Kollias, 1. Papachristodoulos, Rhodes 3, 6–11.5.1997, 265–274.
3. Kasten, D., Zur Druckfestigkeit von Mauersteinen -Eine Standortbestimmung fuer Europa '92. *Bauingenicur*, 1990, **65**, 11–16.
4. Tsioutras, A. A., Hadjitryfonos, E. K., Hatzitrifon, N. K., Aifantis E.C: Mechanical and environmental effects on the domes of the ottoman Bazaar Hammam in Thessaloniki. *Proc. of 4th Int. Symposium on the Conservation*, Ed. Techn. Ch. of Greece 2, 6-11.5.1997, 181–191.
5. Aravantinos, D., An approach to the moisture problem at the church of Saint Nicholas of Orphanus. *Monument & Environment*, 1994, **2**, 19–38 (in Greek).
6. Aifantis, E. C., On The problem of diffusion in solids. *Acta Mech.*, 1980, **37**, 265–296.
7. Unger, D. J. and Aifantis, E. C., Equilibrium of a solute in an elastic continuum — a statistical approach. *Acta Mech.*, 1990, **81**, 227–233.
8. Wilson, R. X. and Aifantis, E. C., On the theory of stress-assisted diffusion I. *Acta Mech*, 1982, **45**, 269–273.
9. Unger, D. J. and Aifantis, E. C., On the theory of stress-assisted-diffusion II. *Acta Mech*, 1983, **47**, 117–151.
10. Unger, D. J., Gerberich, W. W. and Aifantis, E. C., Further remarks on the implications of steady-state stress-assisted diffusion on environmental cracking. *Scripta Metallurgica*, 1982, **16**, 1059–1064.
11. Papadopoulos, G.A., Crack initiation under stress-assisted diffusion. *J. of the Mech. Behav. of Mat.*, 1993, **4**, 141–147 .